Author/s:
Sangeux, M;Passmore, E;Gomez, G;Balakumar, J;Graham, HK

Title:
Slipped capital femoral epiphysis, fixation by single screw in situ: A kinematic and radiographic study

Date:
2014-01-01

Citation:
Sangeux, M., Passmore, E., Gomez, G., Balakumar, J. & Graham, H. K. (2014). Slipped capital femoral epiphysis, fixation by single screw in situ: A kinematic and radiographic study. Clinical Biomechanics, 29 (5), pp.523-530. https://doi.org/10.1016/j.clinbiomech.2014.03.012.

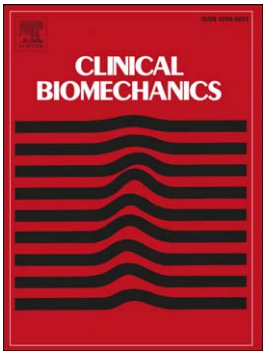


# Slipped Capital Femoral Epiphysis, fixation by single screw *in situ*: A Kinematic and Radiographic Study

Morgan Sangeux, Elyse Passmore, Glenn Gomez, Jitendra Balakumar, H. Kerr Graham

PII: S0268-0033(14)00065-5
DOI: doi: 10.1016/j.clinbiomech.2014.03.012
Reference: JCLB 3770

To appear in: *Clinical Biomechanics*

Received date: 2 December 2013
Revised date: 28 March 2014
Accepted date: 31 March 2014

Please cite this article as: Sangeux, Morgan, Passmore, Elyse, Gomez, Glenn, Balakumar, Jitendra, Kerr Graham, H., Slipped Capital Femoral Epiphysis, fixation by single screw *in situ*: A Kinematic and Radiographic Study, *Clinical Biomechanics* (2014), doi: 10.1016/j.clinbiomech.2014.03.012

# Slipped Capital Femoral Epiphysis, fixation by single screw *in situ*: A Kinematic and Radiographic Study

[1,2,3,*]Morgan Sangeux, MSc, PhD. Senior Biomedical Engineer

[1,2]Elyse Passmore, BEng, MEng. Biomedical Engineer

[1]Glenn Gomez, MBBS. Orthopaedic Registrar

[1]Jitendra Balakumar, MBBS, FRACS, FAOrthA. Consultant Orthopaedic Surgeon

[1,2,4]H. Kerr Graham, MD, FRCS (Ed), FRACS. Professor of Orthopaedic Surgery, Director Hugh Williamson Gait Laboratory

[1] The Royal Children's Hospital

[2] Murdoch Childrens Research Institute

[3] The University of Melbourne, School of Engineering

[4]The University of Melbourne, Department of Paediatrics

Each author certifies that he or she has no commercial associations that might pose a conflict of interest in connection with the submitted article.

** Correspondence to:*

Dr. Morgan Sangeux

The Hugh Williamson Gait Analysis Laboratory

The Royal Children's Hospital

50 Flemington Road, Parkville, VIC 3052

AUSTRALIA

Email: morgan.sangeux@rch.org.au

Word Count: 2952 excluding abstract, legends and references

## Acknowledgments

We thank the staff of The Hugh Williamson Gait Analysis Laboratory and in particular Adrienne Fosang, Senior Clinical Physiotherapist, for their contribution and assistance with data collection. We also thank Susan Donath, biostatistician, for her initial consultation regarding statistical treatment of the data. We acknowledge the help provided by Medical Artist Bill Reid with the illustrations and Mary Sheedy with manuscript preparation.

## Abstract

*Background*

Slipped capital femoral epiphysis is known to produce characteristic deformities in the proximal femur, which affect hip motion and may cause a limp. This paper assessed the 3D gait kinematics in adolescents after single screw fixation of moderate to severe, stable, unilateral slipped capital femoral epiphysis. Our goals were to characterize the 3D kinematic patterns and to investigate the correlation between the severity of radiological deformity and severity of gait disturbance.

*Methods*

This was a retrospective study of patients seen at our institution between 2000 and 2009. Antero-posterior and frog lateral x-rays were reviewed to measure: Southwick's lateral slip angle, the alpha angle of Notzli and Klein's line offset. Quantitative 3D gait data was collected using a state of the art motion capture system. Kinematics waveforms were compared using a functional data analysis version of the t-test.

*Findings*

There were 30 patients with an average age at pinning of 13y (10-17y). Mean gait profile scores were significantly abnormal for slipped side (10.8°) versus sound side (6.8°), slipped side versus normal (5.6°) and sound side versus normal. There was little statistically significant correlation between severity of radiographic deformity and degree of gait disturbance.

*Interpretation*

Major kinematic pattern deviations could be associated with (a) morphology of the proximal femur and potential femoral acetabular impingement problems and (b) leg length discrepancy. Gait analysis was able to quantify the kinematic deviations due to the anatomical deformities.

Word count: 233

Level III Evidence: Retrospective Cohort Study

## Introduction

Slipped capital femoral epiphysis (SCFE) usually presents with pain in the hip or knee and an associated limp. The term SCFE is a misnomer because it is the metaphysis that slips anterosuperior while the epiphysis remains in the acetabulum (Aronsson et al., 2006). Metaphyseal impingement limits hip range of motion in sitting and walking (Parsons et al., 2007). The most common clinical finding during examination of the hip is limitation of internal rotation and flexion. There is usually obligatory external rotation of the hip during flexion (Aronsson et al., 2006; Parsons et al., 2007). The most commonly recognised gait pattern is one of "out toeing" because of inability to internally rotate the hip during gait (Siegel et al., 1991).

Two studies have reported on gait kinematics following SCFE. Song and colleagues reported on gait outcomes in 30 patients with mild to moderate slips (Southwick angle $<50^{o}$) treated by in situ fixation (Song et al., 2004). They reported kinematic abnormalities, which increased in proportion to slip angle on the affected side, when the slip angle was >30°, as well as changes on the unaffected side. Westhoff and colleagues reported detailed three dimensional kinematic abnormalities in 39 skeletally mature patients with mild SCFE, mean Southwick angle 32° (Westhoff et al., 2012). However, their study cohort had been treated by a variety of methods, which might be expected to reduce impingement and improve gait. Neither study reported a summary statistic of gait. Without this it is difficult to appreciate the overall severity of the gait disturbance.

Rab originally described two principal forms of metaphyseal impingement from a three dimensional volume/surface computer model of SCFE in 1999 (Rab, 1999). *Metaphyseal impaction* either causes levering or requires compensatory alteration in hip motion and is associated with acute acetabular cartilage injury. *Metaphyseal inclusion* occurs after remodelling and may lead to delayed acetabular cartilage injury. Since then, the clinical problems of Femoro-Acetabular Impingement (FAI) have been increasingly described in the literature (Beck et al., 2005; Ganz et al., 2003; Mamisch et al., 2009). However, despite the high prevalence of FAI, surgical management of SCFE remains controversial, with little agreement amongst surgeons noted in a recent European survey (Sonnega et al., 2011). One of the factors confounding clinical decision making is the poor correlation between slip severity and symptoms (Aronsson et al., 2006; Dawes et al., 2011; Parsons et al., 2007).

The primary aim of this study was to characterise the 3D kinematic patterns and quantify the magnitude of the gait deviations associated with moderate to severe, unilateral stable slip, after uncomplicated single screw, in situ fixation. A secondary aim was to explore the relationship between kinematic abnormalities and radiographic measures of slip severity and femoro-acetabular impingement (FAI).

## Methods

This was a retrospective cohort study of gait and radiological measures in a group of adolescents and young adults with unilateral, stable, moderate to severe SCFE, managed by single screw in situ fixation.

The study was conducted in the XX Gait Laboratory, the XX Hospital, between 2000 and 2009. The institution's Human Research Ethics Committee (Approval number CA27098) gave ethics approval. No external funding was received in support of this study by any of the authors.

The patients' inclusion criteria for the study were:

1. Unilateral SCFE, confirmed clinically and radiographically, with a lateral slip angle >30$^{o}$ (LSA, method of Southwick, Figure 1.a)
2. Managed by single screw, in situ fixation with no clinical or radiological evidence of complications such as chondrolysis, avascular necrosis, slip progression or infection.
3. No evidence of contralateral slip clinically or radiographically.
4. Three-dimensional gait analysis within 12 months of index surgery.
5. A minimum of three years clinical and radiological follow-up.
6. No interval surgical intervention between index surgery and gait analysis.

Standardised physical examination was conducted according to Gait Laboratory protocols and included measurement of both real and apparent leg length discrepancy using a tape measure. Quantitative kinematic gait data was collected with a state of the art Vicon system (Oxford Metrics, Oxford, United Kingdom) and two AMTI force plates. Reflective markers were applied to the osseous landmarks with use of a standardised procedure. Kinematic data was calculated with use of Plug in Gait (Oxford Metrics, Oxford, United Kingdom) which follows the model originally described by Davis (Davis et al., 1991). At least three strides per side and per patient were selected for kinematics analysis. Normative data for this study was derived from a cohort of 38 children and adolescents (mean 11 years, SD 3, range 4-16) with no gait pathology (NGP) who underwent gait analysis utilising the same standardised procedure as outlined above.

Kinematic waveforms for the pelvis, hips, knees, ankles and foot progression angles were treated as functional data (Ramsay and Silverman, 2005) and included in the analysis. Functional data analysis is a field of statistics that consider such data as varying over a continuum rather than collection of independent points. It is particularly well suited for kinematics data since movement is continuous over time. The curves were converted in functional data using Fourier basis functions (Ramsay et al., 2009) since kinematics traces are considered cyclical and stationary. Functional statistical analysis between kinematics waveforms was performed using a permutation t-test (Ramsay et al., 2009) for the following comparisons: Slipped side versus NGP, Sound side versus NGP and Slipped side versus Sound side with $\alpha < 0.05$.

The Gait Profile Score (GPS) was calculated for each subject as well as Gait Variable Scores (GVS) for nine kinematic parameters (pelvic tilt, pelvic obliquity, pelvic rotation, hip flexion, hip adduction, hip rotation, knee flexion, ankle dorsiflexion and foot progression) (Baker et al., 2009). The nine GVS and the GPS formed the Movement Analysis Profile which is a graphical representation of these data. Each GVS is a measure of the distance of the patient's curve from the corresponding normative curve. The Gait Profile Score is a composite measure of gait quality or summary statistic of gait. It is calculated as the root mean square of the nine kinematic GVSs. The minimal clinically important difference for GPS is 1.6° (Baker et al., 2012). GPS and GVS units are in degrees and the larger the value the more abnormal is the subject's gait.

Antero-posterior and frog lateral radiographs were obtained immediately prior to three dimensional gait analysis and a series of radiographic measurements were made by two of the authors (GG and JB). Measurements were made using Synapse digital radiology software (Fujifilm, 2009, Stamford, CT) and included: The Lateral Slip Angle (LSA, according to the Southwick Method, Figure 1.a), the Alpha Angle of Notzli (Figure 1.b) and Klein's line offset (Figure 1.c) (Dawes et al., 2011; Green et al., 2009; Notzli et al., 2002; Southwick, 1967).

Pearson correlation coefficients were calculated for each possible combination of gait parameter (GVS and GPS) and radiographic measures on the slipped side to examine the correlation between the degree of gait disturbance and the severity of radiographic deformity. Pearson correlation coefficients were also calculated between radiographic measures and a selection of relevant kinematic features: mean pelvic obliquity, mean pelvic rotation, range of hip flexion, maximum hip flexion, maximum hip extension, mean hip adduction in stance, mean hip rotation and mean foot progression angle.

# Results

The study population comprised 30 consecutive patients (17 male, 13 female), mean age 14 years (range 11 to 20 years) with unilateral SCFE and a lateral slip angle >30°, who received in situ fixation. Mean BMI was 26 kg/m$^2$. Fourteen subjects had a BMI within the normal range, five were overweight and 11 were obese. All 30 eligible patients were included in the study and had their radiographic and kinematic data analysed, none were lost to follow-up. Data from physical examination are reported in Table 1. As expected, hip flexion and internal rotation were significantly reduced on the slipped side and external rotation was significantly increased. The mean true leg length discrepancy was 1.5cm short on the slipped side (SD 0.8cm, range 0.0 to 3.0cm). The apparent leg length discrepancy was 1.7cm short on the slipped side (SD 1.1cm, range 0.0cm to 3.5cm).

## 3D Kinematic patterns

Kinematic results of these patients were compared with the no gait pathology (NGP) dataset. Figures 2, 3 and 4 respectively present the Slipped side versus NGP, Sound side versus NGP and Slipped side versus Sound side comparisons. The functional t-test results are presented by solid bar graphs underneath each waveform. Each bar denotes a significant difference ($\alpha$<0.05) between the mean waveforms during the gait cycle.

For the slipped side (Figure 2), the most significant deviations compare to NGP were in the transverse plane with protracted pelvis and externally rotated hip and foot on the slipped side. The coronal plane showed an upward pelvis obliquity in swing on the slipped side. The sagittal plane mainly showed a reduced hip and knee flexion in swing on the slipped side. The sound side showed smaller deviations compare to NGP in the transverse plane (Figure 3). In the coronal plane, the sound hip was more abducted in stance and displayed near normal sagittal gait patterns. The Slip versus Sound comparison showed additional differences (Figure 4). For the slipped side, the pelvis was mostly up, the hip was adducted, hip flexion range was reduced, knee flexion was reduced in mid-stance and mid-swing and ankle dorsiflexion was reduced in late stance and early swing.

### Magnitude of gait deviations

Differences between kinematic data were further explored using the Movement Analysis Profile (MAP). Figure 5 shows the MAP for the sound and slipped sides. The mean GPS for no gait pathology individuals (NGP) is 5.6° (SD 1.4°). The mean GPS for the slipped side was 10.8°, 5.2° different from NGP (95% CI 4.1-6.4, p<0.001) and three times the minimal clinically important difference. The GPS for the sound side was 1.1° greater than (95% CI 0.5-2.0, p=0.0025).

### Radiographic measures and relationship with gait deviations

Radiographic parameters were abnormal on the slipped side for all three measured criteria. Mean LSA on the slipped side was 45° (SD 13°, range 30° to 75°, normal 12°). Klein's line offset measured -6.4mm (SD 8mm, range -27.5mm to +13mm) on the slipped side compared with + 6.8mm (SD 2.4 mm, range +2mm to +15.5mm) on the sound hip (normal is any positive offset) , whilst the mean alpha angle of Notzli of the slipped side measured 114° (SD 13°, range 75° to 146°) compared with 47° (SD 4°, range 38° to 55°) on the sound side (normal Notzli angle 40 to 44°).

Most correlation coefficients between kinematic parameters (gait variables scores or selected gait features) and radiographic measures were low, indicating little correlation between the degree of radiographic deformity and the severity of gait disturbance (Table 2). Some correlation coefficients were significant ($p < 0.05$) with the Slip angle or Klein's line but none with the alpha angle of Notzli. These were, with Klein's line, the pelvic GVS in the coronal plane (coef.=-0.59, p=0.001), the mean pelvic obliquity (coef.=-0.41, p=0.02) and the maximum hip extension (coef.=0.43, p=0.02). Correlation with the slip angle was found for the mean hip adduction in stance (coef.=-0.40, p=0.03).

## Discussion

This is the first study to use functional data analysis to outline differences in cohort gait analysis data. Functional data analysis allows statistical comparison between two sets of curves without the need to parameterize the curves (extremes, range, etc.). This allows to retain all information in the data, amplitude and timing. Functional data analysis is also statistically rigorous, avoiding the pitfalls associated with calculating the difference between curves at discrete time points treated as independent samples (which they are not). As a result, the graph arrays presented on figures 2, 3 and 4 are rigorous and informative, they provide both the timing of the significant differences between waveforms and the differences in shape. This, to the best of our knowledge, is an original contribution.

This is also the first study specifically reporting data in adolescents with moderate to severe SCFE, managed by a single method and including measure of the magnitude of the gait deviations. We found significant gait abnormalities affecting both the slipped and sound side. The kinematic parameters, which showed the greatest deviation from normal, were in the transverse plane; hip rotation and foot progression (Figure 5). The need to externally rotate the hip during walking, to avoid metaphyseal impingement was predicted by Rab from his 3D computer model (Rab, 1999). This result is supported by our study and previous studies (Siegel et al., 1991; Song et al., 2004). We found that the mean external foot progression was much less than the mean external rotation at the hip. This may have implied a compensatory strategy of pelvic protraction to reduce foot progression. We therefore performed a regression analysis between the mean hip rotation and the mean pelvis rotation on the slipped side post-hoc. We found a significant regression ($p<0.0001$; $R^2=0.59$) which

indicates that more severe external hip rotation resulted in a more protracted pelvis on the slipped side. We interpreted this as a tentative step to improve foot positioning in stance and/or cosmesis of gait (Figure 6).

Significant deviations were found in multiple other kinematic parameters, on both the slipped and sound sides, when compared to normal. In the sagittal plane, deviations were noted including reduced ankle dorsiflexion and incomplete knee flexion (Figure 4). Slipped side ankle equinus and sound side knee flexion tend to equalize the functional leg length difference (Siegel et al., 1991; Song et al., 2004; Westhoff et al., 2012). Accordingly, we interpreted these changes as compensations in response to leg length discrepancy.

We also noted an important pattern in the coronal plane, characterized by a decreased range of movement at the hip in the coronal plane and delayed crossover from adduction to abduction of the slipped side compared to normal gait. This was associated with upward pelvic tilt on the slipped side (Figure 4). We interpret these findings as a response to a lateral metaphyseal impingement. Recent studies on the gait kinematics of subjects with non-SCFE FAI report reduced hip range of movement in the coronal plane (Hunt et al., 2013; Kennedy et al., 2009).

These kinematic deviations may be a complex three dimensional limitation of hip movements during gait, which are possibly related to the proximal femoral deformity and subsequent cam-type FAI during critical phases of gait (Casartelli et al., 2011). This secondary cam-type impingement is a well-recognised precursor to hip pain, chondrolabral pathology and premature coxarthrosis (Ganz et al., 2003; Leunig et al., 2000). The characteristic proximal femoral deformity decreases the head-neck offset, increases the femoral head radius of curvature and results in relative retroversion of the femoral head (Jones et al., 1990; Kordelle et al., 2001; Lavigne et al., 2004). The normal smooth arc of motion between the femoral head and acetabulum is disrupted due to the loss of femoral head-neck junction concavity.

A surprising result from the study was the lack of correlation between the degree of radiographic deformity and the severity of kinematic deviations. Whilst previous literature has suggested relationships between increasing degrees of slip angle and severity of gait abnormality in mild slips this was mostly not observed in this study (Song et al., 2004). Some relationships were found between kinematics in the coronal plane and radiographic parameters. However, those relationships represented only a small ($R^2$<0.3) portion of the variance. It was striking to note that the largest gait deviations (pelvis, hip and foot in the transverse plane) did not correlate with radiographic findings. A limitation of this study was the exclusion of patients with mild slips. This may have contributed to the absence of correlation by reducing the range of radiographic abnormalities at the mild end of the spectrum. The reliability of the three radiographic measurements used is relatively good (Green et al., 2009; Mast et al., 2011). However each of these measures is a two-dimensional measure taken from a radiograph at a specific point in time. Very little information exists as to the reliability of these measures, with respect to the positioning of the patient and the hip during capture of the image. It is highly possible that small changes in hip rotation, would have substantial impact on the measurement of these parameters (Lehmann et al., 2013). This is difficult to study because it would necessitate multiple radiographic exposures on the same day. In the future, more sensitive forms of three-dimensional imaging, preferably without ionising radiation, may provide a much better alternative.

We agree with Westhoff and colleagues that three dimensional kinematics is sensitive tool, able to assess even minor degrees of disturbance of hip motion and gait (Westhoff et al., 2012). Conventional radiological measures, on the contrary, are two dimensional and do not predict with any degree of sensitivity, the effects of either the severity of the slip or FAI on hip kinematics and gait kinematics. The effects of SCFE on hip range of motion and gait could not be predicted from slip angle alone nor from Klein's line and the alpha angle of Notzli. Other factors may influence the degree of impingement and gait disturbance such as remodelling on both the femoral and acetabular sides, as well as femoral and acetabular version (Sankar et al., 2011).

Three dimensional kinematics provides an objective description of an individual patient's gait and how the SCFE affects both hip and overall gait function on both the slipped and sound sides. As such it provides a valid tool to assess functional outcomes of SCFE fixation and effects of treatment. A number of patients in this cohort were offered a proximal femoral realignment osteotomy in part based on their three dimensional hip kinematics. To date a small series of patients have had follow-up studies indicating improvements in gait kinematics following realignment osteotomies.

## REFERENCES

Aronsson, D.D., Loder, R.T., Breur, G.J., Weinstein, S.L., 2006. Slipped capital femoral epiphysis: current concepts. The Journal of the American Academy of Orthopaedic Surgeons 14, 666-679.

Baker, R., McGinley, J.L., Schwartz, M., Thomason, P., Rodda, J., Graham, H.K., 2012. The minimal clinically important difference for the Gait Profile Score. Gait & Posture 35, 612-615.

Baker, R., McGinley, J.L., Schwartz, M.H., Beynon, S., Rozumalski, A., Graham, H.K., et al., 2009. The Gait Profile Score and Movement Analysis Profile. Gait & Posture 30, 265-269.

Beck, M., Kalhor, M., Leunig, M., Ganz, R., 2005. Hip morphology influences the pattern of damage to the acetabular cartilage - Femoroacetabular impingement as a cause of early osteoarthritis of the hip. Journal of Bone and Joint Surgery-British Volume 87B, 1012-1018.

Casartelli, N.C., Maffiuletti, N.A., Item-Glatthorn, J.F., Staehli, S., Bizzini, M., Impellizzeri, F.M., et al., 2011. Hip muscle weakness in patients with symptomatic femoroacetabular impingement. Osteoarthritis Cartilage 19, 816-821.

Davis, R.B., Õunpuu, S., Tyburski, D., Gage, J.R., 1991. A gait analysis data collection and reduction technique. Human Movement Science 10, 575-587.

Dawes, B., Jaremko, J.L., Balakumar, J., 2011. Radiographic Assessment of Bone Remodelling in Slipped Upper Femoral Epiphyses Using Klein's Line and the a Angle of Femoral-Acetabular Impingement: A Retrospective Review. Journal of Pediatric Orthopaedics 31, 153-158.

Ganz, R., Parvizi, J., Beck, M., Leunig, M., Notzli, H., Siebenrock, K.A., 2003. Femoroacetabular impingement - A cause for osteoarthritis of the hip. Clinical Orthopaedics and Related Research, 112-120.

Green, D.W., Mogekwu, N., Scher, D.M., Handler, S., Chalmers, P., Widmann, R.F., 2009. A modification of Klein's Line to improve sensitivity of the anterior-posterior radiograph in slipped capital femoral epiphysis. J Pediatr Orthop 29, 449-453.

Hunt, M.A., Guenther, J.R., Gilbart, M.K., 2013. Kinematic and kinetic differences during walking in patients with and without symptomatic femoroacetabular impingement. Clin Biomech (Bristol, Avon) 28, 519-523.

Jones, J.R., Paterson, D.C., Hillier, T.M., Foster, B.K., 1990. Remodeling after Pinning for Slipped Capital Femoral Epiphysis. Journal of Bone and Joint Surgery-British Volume 72, 568-573.

Kennedy, M.J., Lamontagne, M., Beaule, P.E., 2009. Femoroacetabular impingement alters hip and pelvic biomechanics during gait Walking biomechanics of FAI. Gait Posture 30, 41-44.

Kordelle, J., Millis, M., Jolesz, F.A., Kikinis, R., Richolt, J.A., 2001. Three-dimensional analysis of the proximal femur in patients with slipped capital femoral epiphysis based on computed tomography. Journal of Pediatric Orthopaedics 21, 179-182.

Lavigne, M., Parvizi, J., Beck, M., Siebenrock, K.A., Ganz, R., Leunig, M., 2004. Anterior femoroacetabular impingement Part I. Techniques of joint preserving surgery. Clinical Orthopaedics and Related Research, 61-66.

Lehmann, T.G., Vetti, N., Laborie, L.B., Engesaeter, I.O., Engesaeter, L.B., Rosendahl, K., 2013. Intra- and inter-observer repeatability of radiographic measurements for previously slipped capital femoral epiphysis at skeletal maturity. Acta Radiologica 54, 587-591.

Leunig, M., Casillas, M.M., Hamlet, M., Hersche, O., Notzli, H., Slongo, T., et al., 2000. Slipped capital femoral epiphysis - Early mechanical damage to the acetabular cartilage by a prominent femoral metaphysis. Acta Orthopaedica Scandinavica 71, 370-375.

Mamisch, T.C., Kim, Y.J., Richolt, J.A., Millis, M.B., Kordelle, J., 2009. Femoral Morphology Due to Impingement Influences the Range of Motion in Slipped Capital Femoral Epiphysis. Clinical Orthopaedics and Related Research 467, 692-698.

Mast, N.H., Impellizzeri, F., Keller, S., Leunig, M., 2011. Reliability and Agreement of Measures Used in Radiographic Evaluation of the Adult Hip. Clinical Orthopaedics and Related Research 469, 188-199.

Notzli, H.P., Wyss, T.F., Stoecklin, C.H., Schmid, M.R., Treiber, K., Hodler, J., 2002. The contour of the femoral head-neck junction as a predictor for the risk of anterior impingement. J Bone Joint Surg Br 84, 556-560.

Parsons, S.J., Barton, C., Banerjee, R., Kiely, N.T., 2007. Slipped upper femoral epiphysis. Current Orthopaedics 21, 215-228.

Rab, G.T., 1999. The geometry of slipped capital femoral epiphysis: Implications for movement, impingement, and corrective osteotomy. Journal of Pediatric Orthopaedics 19, 419-424.

Ramsay, J., Silverman, B.W., 2005. Functional data analysis, 2nd edition ed. Springer.

Ramsay, J.O., Hooker, G., Graves, S., 2009. Functional Data Analysis with R and MATLAB. Use R, 1-207.

Sankar, W.N., Brighton, B.K., Kim, Y.J., Millis, M.B., 2011. Acetabular morphology in slipped capital femoral epiphysis. J Pediatr Orthop 31, 254-258.

Siegel, D.B., Kasser, J.R., Sponseller, P., Gelberman, R.H., 1991. Slipped Capital Femoral Epiphysis - a Quantitative-Analysis of Motion, Gait, and Femoral Remodeling after Insitu Fixation. Journal of Bone and Joint Surgery-American Volume 73A, 659-666.

Song, K.M., Halliday, S., Reilly, C., Keezel, W., 2004. Gait abnormalities following slipped capital femoral epiphysis. Journal of Pediatric Orthopaedics 24, 148-155.

Sonnega, R.J., van der Sluijs, J.A., Wainwright, A.M., Roposch, A., Hefti, F., 2011. Management of slipped capital femoral epiphysis: results of a survey of the members of the European Paediatric Orthopaedic Society. J Child Orthop 5, 433-438.

Southwick, W.O., 1967. Osteotomy through the lesser trochanter for slipped capital femoral epiphysis. J Bone Joint Surg Am 49, 807-835.

Westhoff, B., Ruhe, K., Weimann-Stahlschmidt, K., Zilkens, C., Willers, R., Krauspe, R., 2012. The gait function of slipped capital femoral epiphysis in patients after growth arrest and its correlation with the clinical outcome. International Orthopaedics 36, 1031-1038.

## Figures and Figure legends (six figures)

**Figure 1:**

a) The Lateral Slip Angle (LSA) of Southwick: The value for the normal hip is 12°. A mild slip is defined as an LSA <30°, a moderate slip is 30°-50°, and a severe slip is >50°.

b) Alpha ($\alpha$) angle of Notzli. The angle is measured on a lateral radiograph between the midline of the femoral neck and the point at which the lateral femoral head-neck junction deviates from a circle. The normal $\alpha$ angle is 40-44°. Angles >50°-55° indicate femoral acetabular impingement (FAI).

c) Klein's line: Klein's line is measured on an anterior-posterior (AP) radiograph of the hip as the displacement between the line running along the superior aspect of the neck and a line through the edge of the epiphysis. The normal Klein's line is positive i.e. the epiphysis projects proximal or above the line along the neck. Negative values measured in millimetres of displacement are abnormal. d is negative on the picture.

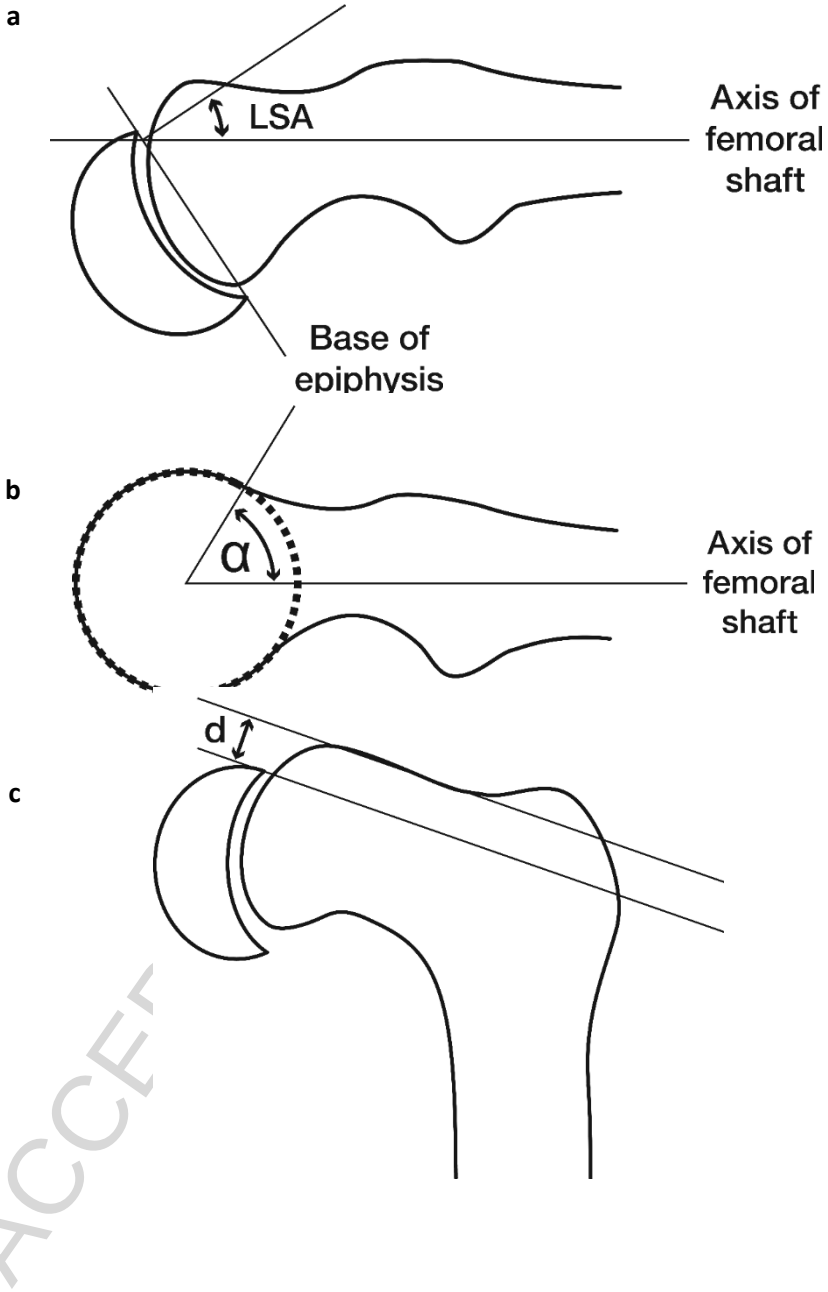


**Fig1**

**Figure 2:** Kinematic comparison graph arrays between the patients' slipped side and the no gait pathology (NGP) groups mean. Kinematics waveform comparisons are presented for the pelvis, hip, knee, ankle and foot in the three planes for a total of twelve graphs. Each graph presents the slipped side group mean (± 1 standard deviation) in red hashes and the NGP group mean (± 1 standard deviation) in grey. A bar chart is also presented underneath each graph. The bar chart presents the result of the functional data analysis t-test on the waveforms mean. Only the time instants denoted by the black bars denote significant differences ($\alpha < 0.05$) between waveform means.

The most notable deviations were in the transverse plane with differences found over the whole gait cycle for the pelvic rotation (slipped side protracted compare to NGP), the hip rotation (slipped externally rotated compare to NGP) and foot progression angle (externally rotated compare to NGP). The sagittal plane showed milder deviations, the slipped side showed increased pelvic tilt in late stance, reduced hip flexion in late swing, reduced knee flexion in mid-stance and most of the swing phase and reduced ankle dorsiflexion in late stance. The coronal plane displayed an upward pelvic obliquity for the slipped side compare to NGP in the swing phase.

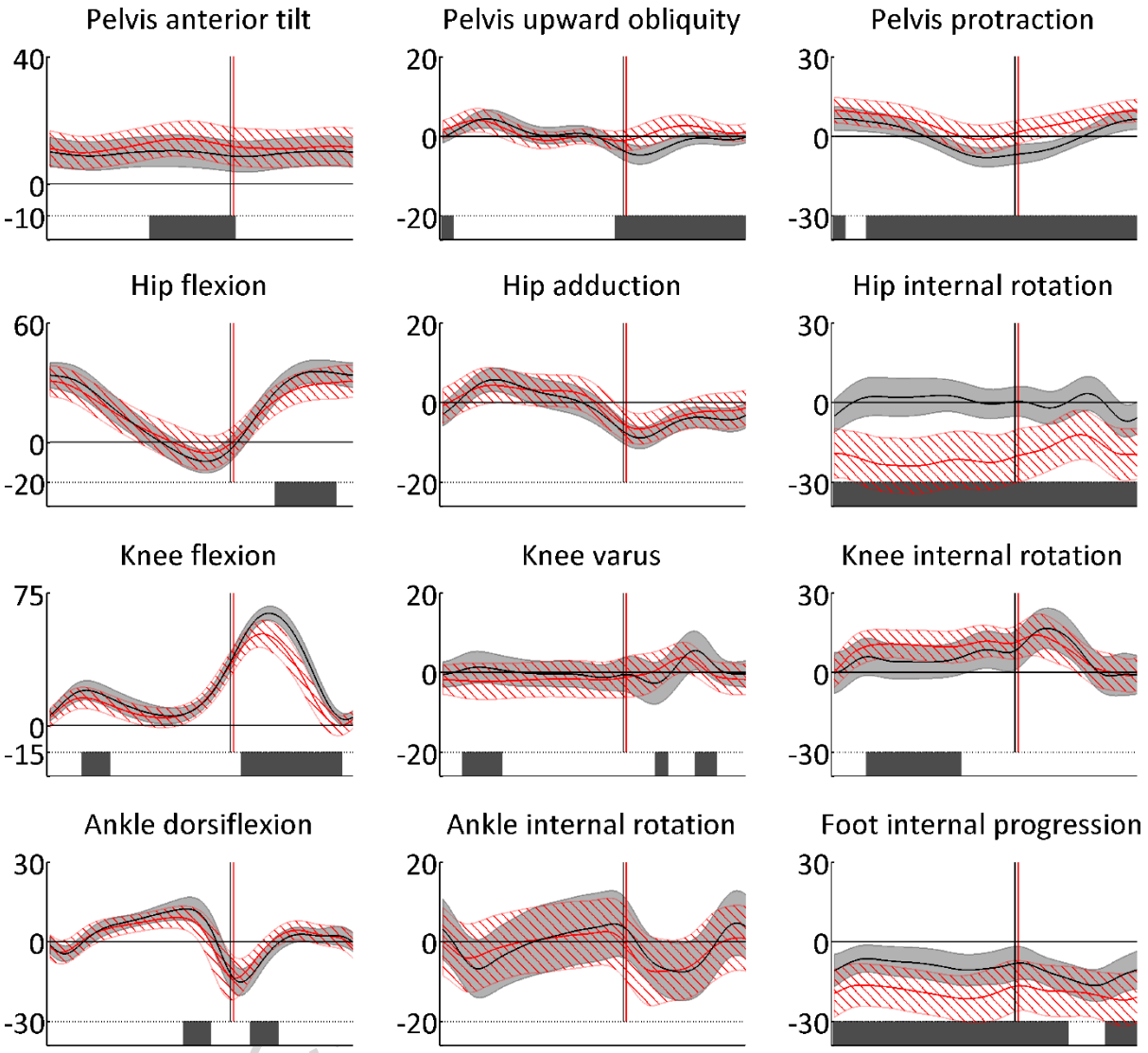


**Fig2**

**Figure 3**: Kinematic comparison graph arrays between the patients' sound side and the no gait pathology (NGP) groups mean. Kinematic waveform comparisons are presented for the pelvis, hip, knee, ankle and foot in the three planes for a total of twelve graphs. Each graph presents the sound side group mean (± 1 standard deviation) in blue hashes and the no gait pathology group mean (± 1 standard deviation) in grey. A bar chart is also presented underneath each graph. The bar chart presents the results of the functional data analysis t-test on the waveforms mean. Only the time instants denoted by the black bars denote significant differences ($\alpha < 0.05$) between waveform means.

The sagittal plane was only marginally different from the NGP group. The coronal plane showed a downward pelvic tilt in stance for the sound side compare to NGP and a slightly reduced hip adduction in stance. Milder (than for the slipped side) deviations were noted for the sound side compared to the NGP group for the transverse plane, these included pelvic retraction and slight external rotation of the hip in mid-stance.

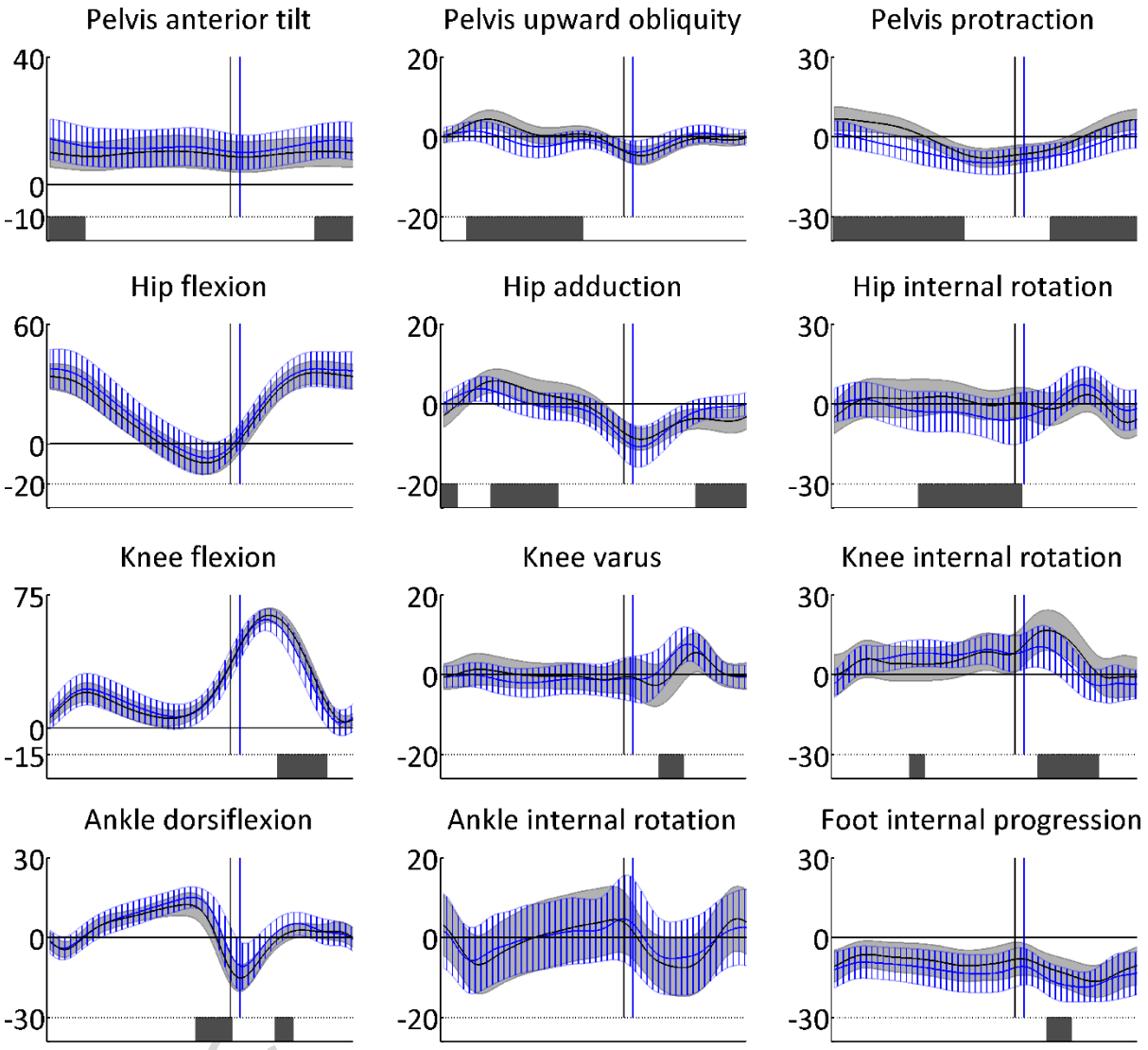


**Fig3**

**Figure 4**: Kinematic comparison graph arrays between the patients' slipped side and the patients' sound side groups mean. Kinematic waveform comparisons are presented for the pelvis, hip, knee, ankle and foot in the three planes for a total of twelve graphs. Each graph presents the slipped side group mean (± 1 standard deviation) in red hashes and sound side group mean (± 1 standard deviation) in blue hashes. A bar chart is also presented underneath each graph. The bar chart presents the results of the functional data analysis t-test on the waveforms mean. Only the time instants denoted by the solid color (green, orange, black) bars denote significant differences ($\alpha < 0.05$) between waveform means.

The most notable deviations were in the transverse plane with differences found over the whole gait cycle for pelvic rotation (slipped protracted compare to sound), hip rotation (slipped externally rotated compare to sound) and foot progression angle (slipped externally rotated compare to sound). The sagittal plane showed marked deviations at some instants of the gait cycle, the slipped hip flexion was reduced in early stance and late swing leading to a reduced range, the slipped knee flexion was reduced in mid-stance and mid-swing phases and the slipped ankle showed reduced dorsiflexion in late stance, early swing. The coronal plane displayed an upward pelvic obliquity for the slipped side compare to sound for most of the gait cycle and slipped side hip adduction increased compare to sound from mid-stance to mid-swing.

The interpretable gait deviations have been classified in two groups and highlighted by green or orange significant difference bars. We attributed the green group deviations to the shape of the proximal femur on the slipped side and possible Femoral Acetabular Impingement problems. We attributed the pelvis protraction to a voluntary compensation to improve alignment of the foot. We attributed the orange group deviations to the leg length discrepancy (slipped shorter than sound, Table 1) problem.

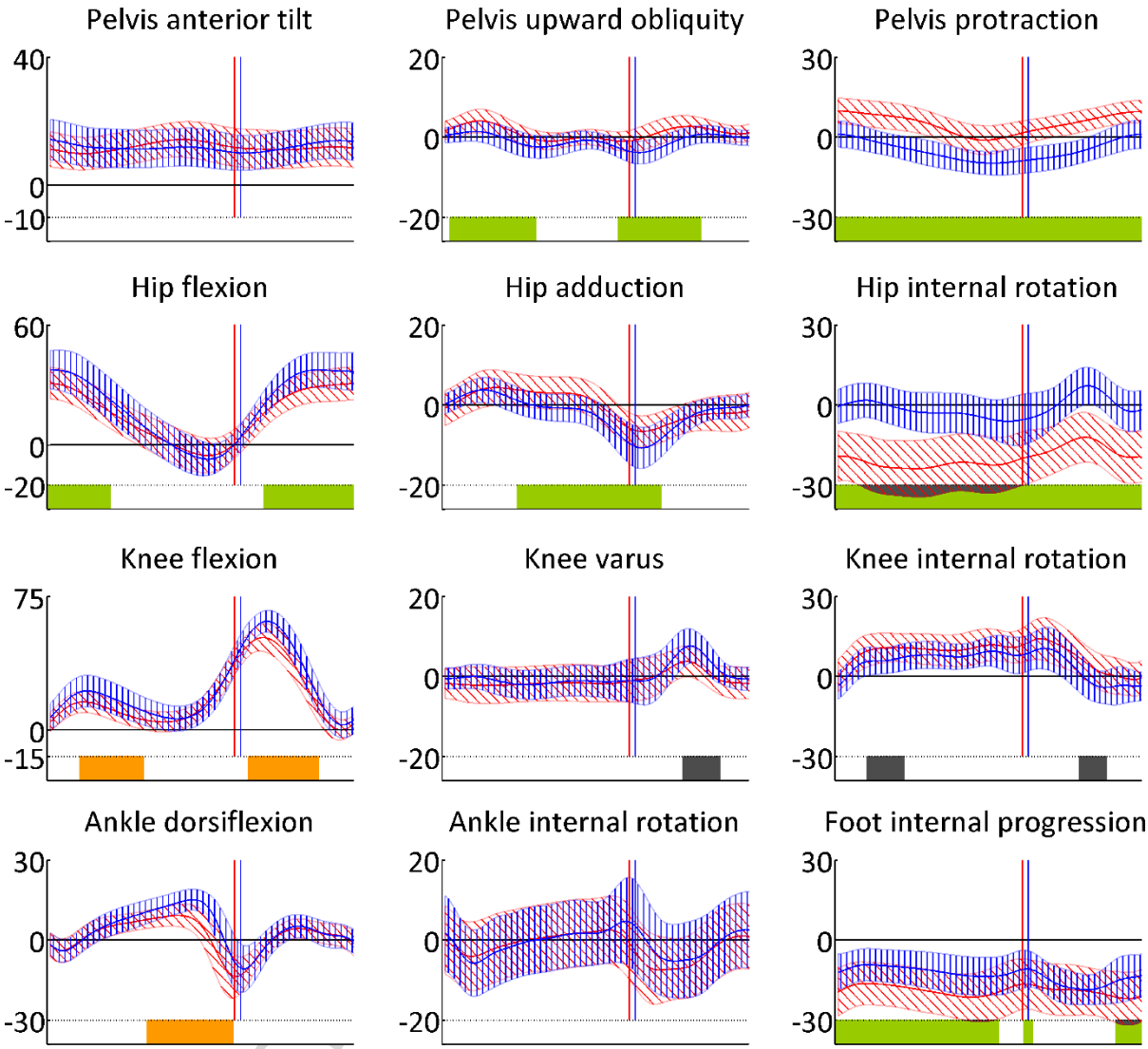


**Fig4**

**Figure 5**: Movement Analysis Profile (MAP) for the whole cohort in comparison to the control group, with no gait pathology (NGP). The first nine bar clusters indicate the individual Gait Variable Scores (GVS) for nine kinematic parameters and the last shows the Gait Profile Score (GPS). For each group of results the clear bar is the sound side, the shaded bar is the slipped side and the black bars are the normal mean from individuals with no gait pathology (NGP).

Significant statistical differences ($\alpha$<0.05) between the slipped/sound side versus NGP are indicated by †. Significant statistical difference between the slipped versus the sound side are indicated by a curly brace and *. The red line indicates the minimal clinically important difference for GPS.

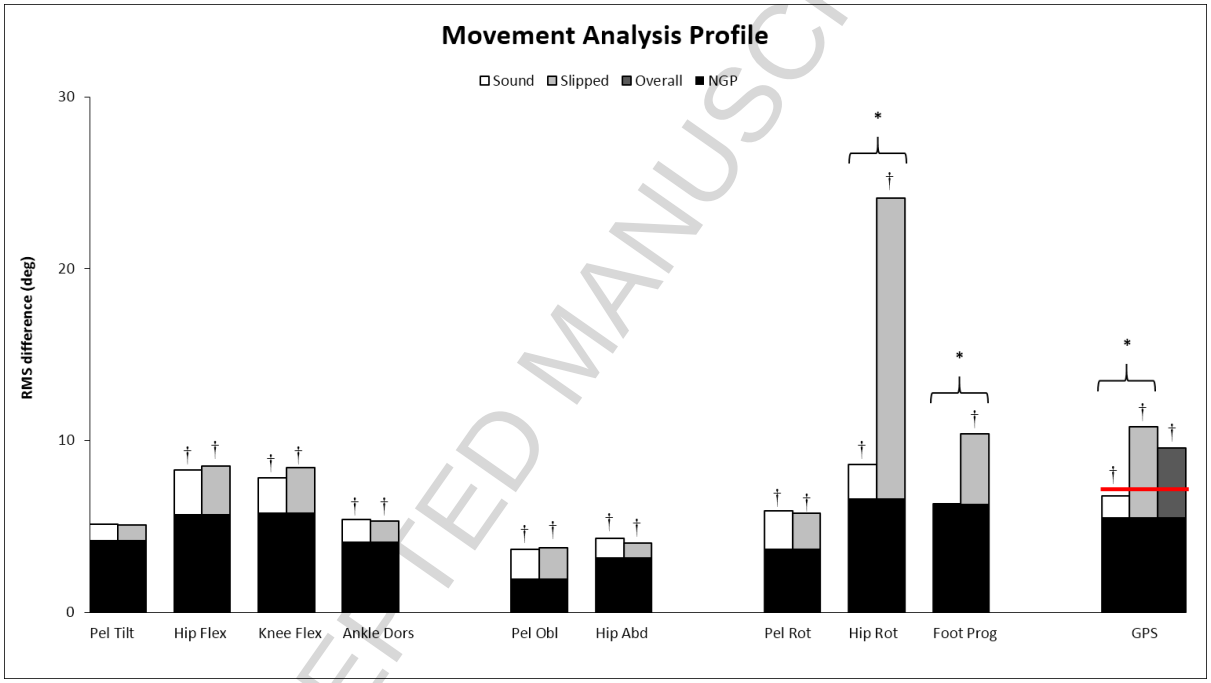


fig5

**Figure 6:** Principal gait deviations and secondary compensations in the coronal and transverse planes associated with SCFE.

In severe high grade slip, with lateral impingement, hip abduction is reduced. This results in an upward pelvic obliquity which results in an apparent limb length discrepancy. In the transverse plane, the external foot progression may be compensated by pelvic protraction as a compensatory mechanism to control the foot progression angle in the presence of an anterolateral metaphyseal block to internal hip rotation.

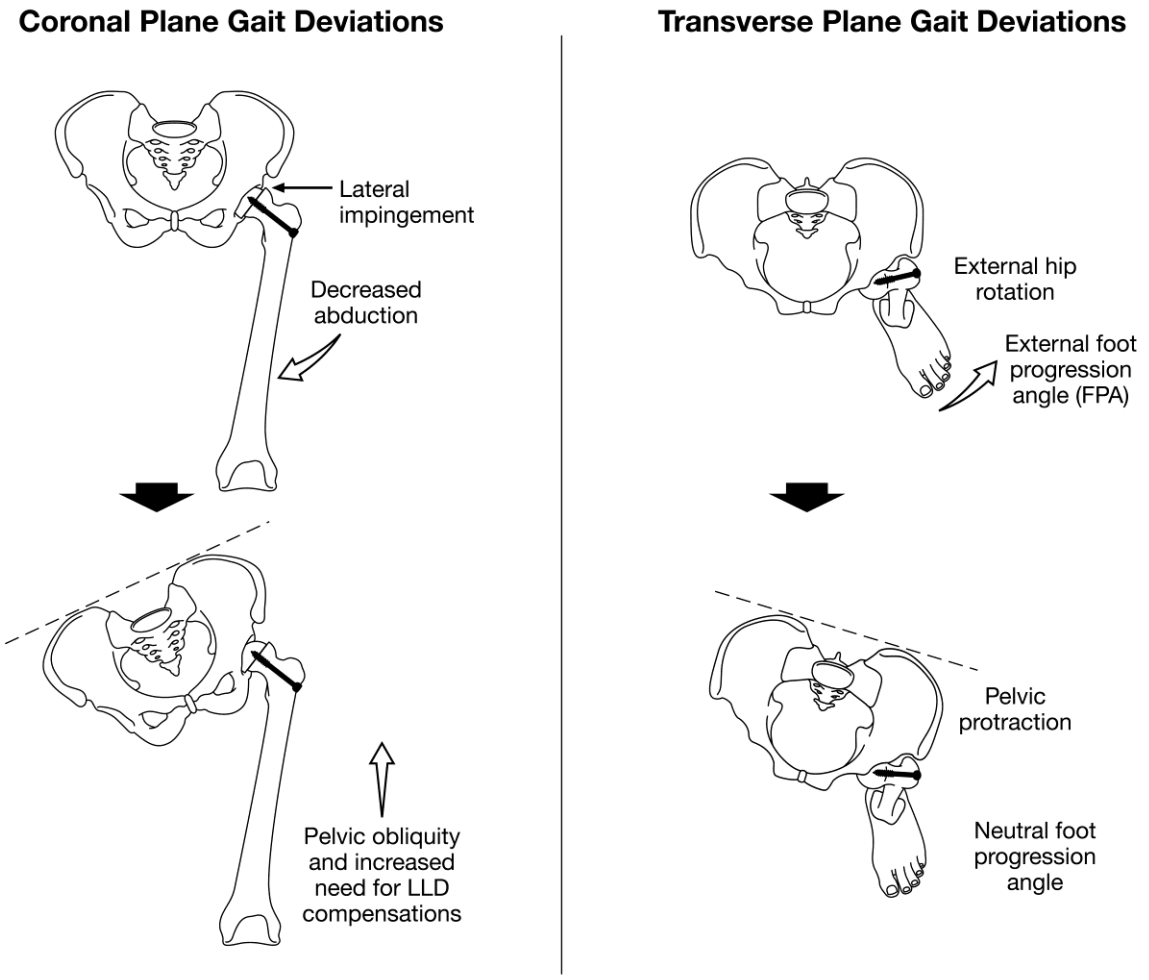


Fig6

# Tables (two tables)

**Table 1:** Physical examination measures

| | **SLIPPED SIDE** Mean (SD, Range) | **SOUND SIDE** Mean (SD, Range) | **SIGNIFICANCE** P value |
|---|---|---|---|
| **Hip flexion** | **99° (24°, 40° to 135°)** | **118° (10°, 97° to 135°)** | **0.001** |
| Hip extension (Thomas) | 5° (8°, - 7° to 25°) | 6° (8°, - 8° to 22°) | 0.63 |
| Hip extension (Staheli) | 6° (11°, - 7° to 40°) | 2° (8°, -11° to 20°) | 0.18 |
| Hip abduction | 16° (6°, 5° to 30°) | 14° (5°, 5° to 20°) | 0.34 |
| **Hip internal Rotation** | **5° (17°, - 27° to 39°)** | **36° (16°, -17° to 55°)** | **<0.001** |
| **Hip external Rotation** | **54° (18°, 26° to 90°)** | **42° (18°, 20° to 85°)** | **0.01** |
| **Leg length discrepancy** | **15mm short on slipped side (8mm, 0 to 30mm)** | | **0.001** |

The minus sign (-) indicates a flexion deformity at the hip or a fixed external rotation deformity. Significant differences between slipped side and sound side at $p < 0.05$ are indicated in bold.

**Table 2:** Correlations between radiographic and kinematic features. For each correlation we present the Pearson's coefficient and the p value. p values < 0.05 are highlighted in bold and listed (a, b, c, d) below for further explanation. However, interpretation of p values should be careful since we tested many correlations and therefore increased the probability of finding a significant correlation (p < 0.05) by chance.

a) Decreasing Klein's line offset (more abnormal) was correlated with increased deviation from normal at the pelvis in the coronal plane

b) Decreasing Klein's line offset was correlated with increased mean pelvic obliquity

c) Decreasing Klein's line offset was correlated with decreased maximum hip extension

d) Increasing Slip angle (more abnormal) was correlated with reduced mean hip adduction in stance

| | | Slip angle | | Alpha angle | | Klein's line | |
|---|---|---|---|---|---|---|---|
| | | Coef. | p | Coef. | p | Coef. | p |
| MAP | Pelvic sagittal | -0.04 | 0.83 | -0.16 | 0.41 | 0.22 | 0.24 |
| | **Pelvic coronal** | 0.00 | 0.99 | 0.05 | 0.79 | **-0.59[a]** | **0.001** |
| | Pelvic transverse | -0.19 | 0.32 | -0.10 | 0.61 | -0.01 | 0.97 |
| | Hip sagittal | -0.23 | 0.23 | 0.10 | 0.59 | 0.13 | 0.50 |
| | Hip coronal | 0.14 | 0.49 | 0.04 | 0.83 | -0.29 | 0.12 |
| | Hip transverse | -0.11 | 0.58 | 0.17 | 0.37 | -0.31 | 0.09 |
| | Knee sagittal | -0.08 | 0.69 | 0.33 | 0.07 | -0.32 | 0.08 |
| | Ankle sagittal | 0.30 | 0.11 | 0.36 | 0.05 | 0.03 | 0.87 |
| | Foot transverse | -0.15 | 0.45 | 0.27 | 0.14 | -0.13 | 0.49 |
| | GPS | -0.17 | 0.37 | 0.25 | 0.18 | -0.27 | 0.15 |
| Kinematic features | **Mean pelvis obliquity** | -0.18 | 0.35 | -0.13 | 0.50 | **-0.41[b]** | **0.02** |
| | Mean pelvis potation | -0.32 | 0.09 | -0.08 | 0.69 | -0.06 | 0.76 |
| | Range hip flexion | 0.01 | 0.98 | -0.35 | 0.06 | 0.28 | 0.13 |
| | Max hip flexion | 0.04 | 0.83 | 0.02 | 0.94 | -0.26 | 0.17 |
| | **Max hip extension** | 0.04 | 0.86 | 0.24 | 0.20 | **0.43[c]** | **0.02** |
| | **Mean hip adduction (stance)** | **-0.40[d]** | **0.03** | -0.18 | 0.33 | -0.23 | 0.23 |
| | Mean hip rotation | 0.12 | 0.54 | -0.16 | 0.41 | 0.27 | 0.14 |
| | Mean foot progression | 0.35 | 0.07 | -0.26 | 0.17 | 0.10 | 0.59 |